Spatial Characterization of the Tumor Microenvironment with Cell DIVE Multiplexed Imaging and HALO Quantitative Image Analysis

Amber L Ortiz, PhD[1], Michael Smith, PhD[2], Lisa Arvidson[3], Ines Nearchou, PhD[1], Douglas Bowman[1] and Arindam Bose, PhD[4]

[1]Indica Lab, Albuquerque, NM, [2]Leica Microsystems, Buffalo Grove, IL, [3]Cell Signaling Technology, Danvers, MA, [4]Leica Microsystems, Waltham, MA

BACKGROUND

Understanding cellular and molecular drivers of cancer cell aggression in tumors is essential to targeted therapy development and deployment to patients. Multiplex immunofluorescence and digital pathology analysis have become the standard protocol in research facilities to probe and understand these biological relationships. Antibody-based multiplex immunofluorescence can quantify hundreds of proteins in tumor cells to study how protein localization changes in pathogenic cells, while AI-based analysis methods deliver unprecedented insight into biological processes, both in fundamental cell biology and translational research. These technological advances have become important in tumor microenvironment (TME) immune profiling. Here we identified heterogeneity in exhausted T cells and used this finding to explore the association between these cells and checkpoint-blockade therapies. Identifying biomarkers that predict response to checkpoint blockade may be an important predictor of the response to immunotherapies.

METHODS

A tissue micro array (TMA) containing 40 tumor tissues from 27 different anatomic sites was stained using 30 antibodies from Cell Signaling Technology (CST) and imaged using the Cell DIVE Multiplex Imaging Solution from Leica Microsystems. The cores were then analyzed using HALO® image analysis platform from Indica Labs to better understand the TME.

CELL DIVE MULTIPLEXED IMAGING WORKFLOW

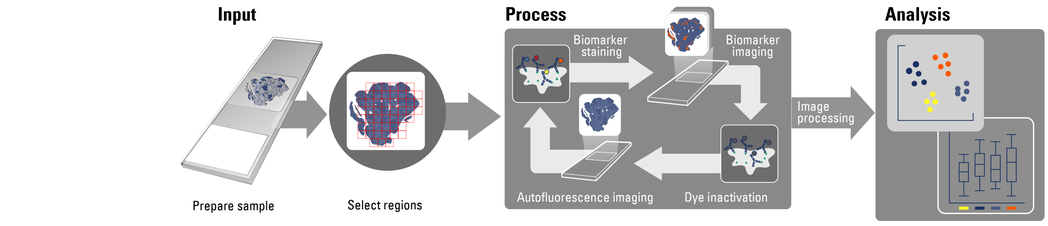

CST® ANTIBODY SELECTION

Cat. #	Antibody	Clone	Conjugate	Conc. (ug/mL)	Dil.
9854S	Vimentin	D21H3	AF_488	200	1:100
34105S	SMA	D4K9N	AF_488	125	1:100
4523S	Panck	C11	AF_488	100	1:100
3478S	Panck	C11	AF_555	32	1:100
23308S	CD68	D4B9C	AF_555	4.5	1:100
*	SMA	1A4	AF_488	100	1:100
*	Sox9	D8G8H	AF_488	100	1:100
*	ATP1A1	D4Y7E	AF_488	100	1:100
*	CD79A	D1X5C	AF_555	100	1:100
*	CD3ε	D7A6E™	AF_555	100	1:100
*	CD20	E7B7T	AF_647	100	1:100
*	CD163	D6U1J	AF_647	100	1:100
*	Ki-67	D2H10	AF_647	100	1:100
*	CD8α	D8A8Y	AF_750	100	1:100
*	CD45	D9M8I	AF_750	100	1:100
*	PD-1	D4W2J	AF_750	100	1:100

Cat. #	Antibody	Clone	Conjugate	Conc. (ug/mL)	Dil.
*	Vimentin	D21H3	AF_750	100	1:100
*	FoxP3	D2W8E™	AF_647	500	1:100
*	CD4	D7D2Z	AF_555	200	1:100
*	CD56	E7X9M	AF_647	200	1:100
*	PDL-1	E1L3N	AF_647	200	1:100
*	CTLA-4	E2V1Z	AF_647	200	1:100
*	CD11B	D6X1N	AF_750	200	1:100
*	LAG3	D2G4O	AF_750	200	1:100
*	GZMB	D6E9W	AF_555	200	1:100
3655	GFAP	GA5	AF_488	50	1:100
78226	TIM-3	D5D5R	AF_647	100	1:100
61255	CD31	89C2	AF_555	47	1:100
5108	EGFR	D38B1	AF_555	50	1:100
7497	pNDRG1	D98G11	AF_647	25	1:100
3906	GAPDH	14c10	AF_488	100	1:100
2866	SURVIVIN	71G4B7	AF_647	50	1:100
5067	SOX2	D6D9	AF_647	25	1:100

TMA MAP for SELECTED CORES

Ref. No	Position	Sex	Age	Anatomic Site	Pathology	Grade	Stage
F05-1029	C05	F	40	Intestine, small intestine	Normal	null	null
F05-1325	C06	F	18	Intestine, small intestine	Adenoma	null	null
F06-1201	C07	F	57	Intestine, small intestine	Adenocarcinoma	II	T2N0M0
F06-1979	C08	F	27	Intestine, colon	Normal	null	null
F05-1404	C09	M	57	Intestine, colon	Adenoma	null	null
F06-1539	C10	M	56	Intestine, colon	Adenocarcinoma	I	T3N0M0
F06-1336	C11	M	89	Intestine, colon	Adenocarcinoma	II	T2N0M0
F06-0502	C12	F	43	Intestine, colon	Adenocarcinoma	III	T3N0M0
F05-1744	D01	M	61	Intestine, rectum	Normal	null	null
F06-1040	D02	M	40	Intestine, rectum	Adenocarcinoma	I	T3N0M0
F06-1023	D03	M	38	Intestine, rectum	Adenocarcinoma	II	T3N1M0
F06-1111	D04	M	50	Intestine, rectum	Adenocarcinoma	III	T3N1M0
F05-1783	D08	M	43	Liver	Normal	null	null
F06-1326	D09	M	26	Liver	Hepatocellular carcinoma	I	T2N0M0
F06-1173	D10	M	40	Liver	Hepatocellular carcinoma	II	T2N0M0
F07-1295	D11	M	53	Liver	Hepatocellular carcinoma	I	T2N0M0
F06-1802	D12	M	41	Liver	Hepatocellular carcinoma	III	T2N0M0
F06-1920	E01	M	58	Lung	Normal	null	null
F06-1385	E02	M	59	Lung	Squamous cell carcinoma	II	T2N2M0
F06-1701	E03	M	62	Lung	Squamous cell carcinoma	II~III	T2N2M0
F06-1206	E04	M	72	Lung	Adenocarcinoma	III	T2N2M0
F06-1739	E05	M	19	Lung	Small cell carcinoma	null	T3N0M0

HALO® and HALO AI IMAGE ANALYSIS WORKFLOW of CELL DIVE IMAGES

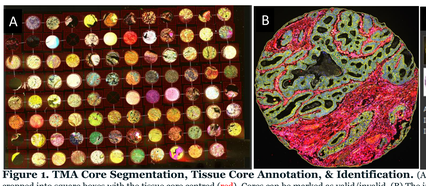

Figure 1. TMA Core Segmentation, Tissue Core Annotation, & Identification. (A) The cores are automatically detected and cropped into square boxes with the tissue core centred (red). Cores can be marked as valid/invalid. (B) The individual tissue cores can be automatically annotated using the flood tool. Manual edits as well as additional exclusion annotations can be made. (C) Manifest data information can be added to the TMA block/core and will be exported with TMA results.

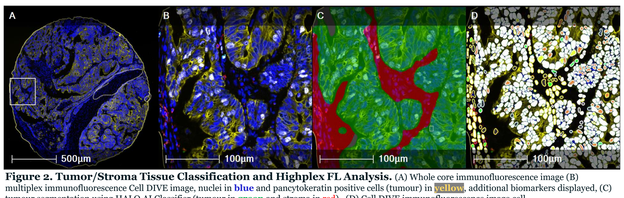

Figure 2. Tumor/Stroma Tissue Classification and Highplex FL Analysis. (A) Whole core immunofluorescence image (B) multiplex immunofluorescence Cell DIVE image, nuclei in blue and pancytokeratin positive cells (tumour) in yellow, additional biomarkers displayed, (C) tumour segmentation using HALO AI Classifier (tumour in green and stroma in red). (D) Cell DIVE immunofluorescence image cell classification/analysis mark-up (colocalization) using the Highplex FL module.

RESULTS

We found that most tumors had an increase in expression of vimentin, alpha-SMA, survivin, and Ki67 with respect to non-tumor tissues. These markers are often upregulated in aggressive tumors and are responsible for increased cell survival, angiogenesis, and invasiveness. These tissues also expressed PD-1 and PD-L1 checkpoint signaling biomarkers at lower levels suggesting a potentially reduced response to immunotherapy. We found that some cancer types, such as esophageal cancer, squamous cell carcinoma, breast, adenocarcinoma and head-and-neck tended to have higher levels of LAG-3 and TIM-3 expression than normal tissue. Higher levels of LAG-3 and TIM-3 expression in T cells has been associated with poor prognosis and could inhibit the immune response to cancer. Anti-cancer treatment targeting TIM-3 and LAG3 could benefit patients undergoing immunotherapy. Further in-depth analysis such as proximity of specific cell types to tumor cells as well as the infiltration of cell types such as immune cells into the tumor regions can help lead to better detection of valuable biomarkers. Novel combinations of these inhibitors with the current standard of care might be a promising approach to increase progression-free survival.

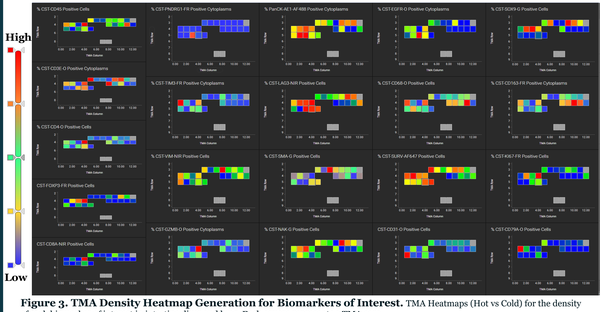

Figure 3. TMA Density Heatmap Generation for Biomarkers of Interest. TMA Heatmaps (Hot vs Cold) for the density of each biomarker of interest in intestine, liver and lung. Each square represents a TMA core.

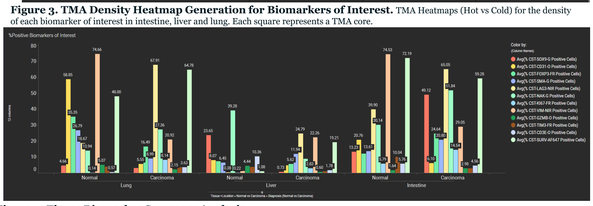

Figure 4. Tissue Biomarker Summary Analysis. %Positive Biomarkers of interest within the Normal and Carcinoma regions of Lung, Liver, and Intestine.

Figure 5. Normal vs Carcinoma Tissue Biomarkers of Interest. %Positive SOX9, VIM, CD31, TIM3, LAG3, CD3, KI67, & SURV Biomarkers with noticeable discordance between Normal and Carcinoma groups.

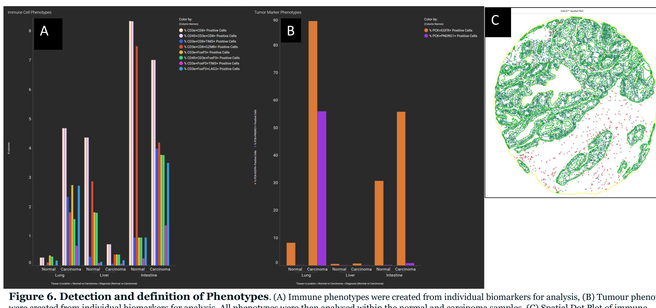

Figure 6. Detection and definition of Phenotypes. (A) Immune phenotypes were created from individual biomarkers for analysis, (B) Tumour phenotypes were created from individual biomarkers for analysis. All phenotypes were then analysed within the normal and carcinoma samples. (C) Spatial Dot Plot of immune phenotype positive cells and tumour regions (green).

PROXIMITY ANALYSIS

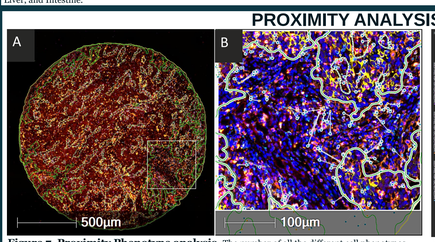

Figure 7. Proximity Phenotype analysis. The number of all the different cell phenotypes within a specified radius of a tumour cell (in this case 250 µm) is calculated. Full core image (A) and zoom-in into tumour border area (B)

Figure 8. Histogram of the number of the different phenotypes within a 250 µm radius from any tumour cell.

INFILTRATION ANALYSIS

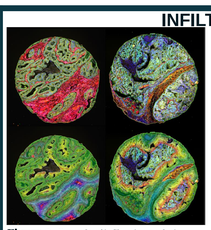

Figure 9. Example of infiltration analysis within the TMA core on the tumor interface. Infiltration analysis is done 150 µm on either side of the tumor boundary at 30 µm bins.

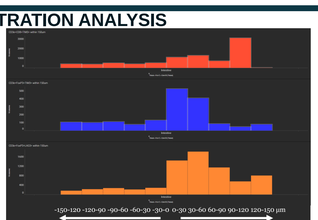

Figure10. Histogram of the density (per mm^2) of the immune phenotypes within a 150µm range from the tumour interface of intestinal carcinoma cores.

CONCLUSIONS

A combined workflow using CST antibodies, the Cell DIVE platform for highly multiplex staining and immunofluorescence imaging combined with HALO quantitative image analysis delivers a comprehensive solution for exploring the immune landscape of tumor tissue. Here, we find differential expression of markers of cancer aggression and immune cell responsiveness in a variety of cancer types. Using this critical information could help guide immunotherapy development and clinical trial stratification.

REFERENCES

• MTU951. Cancers/tumors of 40 types, 95 cases (1.5mm). (Pantomics, INC)

Abstract: 111

Correspondence: aortiz@indicalab.com, celldive@leica-microsystems.com, support@cellsignalling.com